

# Noncontact Position Estimation Device with Optical Sensor and Laser Sources for Mobile Robots Traversing Slippery Terrains

Isaku Nagai\*, Keigo Watanabe\*, Keiji Nagatani\*\*, and Kazuya Yoshida\*\*

\*Dept. of Intelligent Mechanical Systems, Okayama Univ., Japan

\*\*Dept. of Aerospace Engineering, Tohoku Univ., Japan

**Abstract**—This paper describes the development of a sensing device that can be used to estimate the position of mobile robots on slippery terrains. The device consists of an optical sensor designed for a computer mouse and dual laser light sources for generating a laser speckle pattern. It detects the motion of a moving surface at a large distance from the surface, from 80 mm to 300 mm, by tracking the laser speckle pattern. The use of dual laser light sources makes the tracking robust for both large distances from the ground and different surface materials. Some fundamental experiments validated the performance of the device, which tracked surfaces of different materials with high accuracy under various height conditions. Finally, the device was mounted on our mobile robot, and simple experiments were conducted on a slippery sandy terrain to evaluate the usefulness of the device as a noncontact odometry system.

## I. INTRODUCTION

Moon/planetary rovers and rescue robots are typically fitted with wide wheels or tracks so that they can traverse rough or sandy terrains such as the regolith on the moon's surface, debris fields, or rocky terrains. However, because of the slippage between mechanisms and loose terrains, it is almost impossible for such a mobile robot to use wheeled odometry to estimate its position. To provide an effective odometry system for robots with such slippage problems, some noncontact type odometry systems have been proposed. One approach is to use the optical sensor designed for a computer mouse. The characteristics of conventional optical sensors have been investigated for use in applications other than computer mice, such as mobile robots [1-2]. Some positioning methods have been proposed that use optical sensors to measure the translation and rotation displacements of the moving surface under a mobile robot [3-5]. Optical sensors can be used not only for mobile robots but also for measuring rotational motions such as those of a rotary encoder [6]. The dual use of the sensor contributes to an improvement in the robot posture accuracy [7-9]. Such positioning methods are independent of the locomotion mechanism, allowing an optical sensor to be applied to the position estimation of a Mecanum wheel robot [10]. This type of sensing device is so compact that it can also be applied not only to the motion estimation of a real car [11] but also to a small desktop robot [12]. A lens of a certain focal length with an optical sensor can be used to estimate the motion with a

large height from the object surface [13]. However, in all of the above applications, the distance between the sensor and the surface is limited to a short range because the sensor was originally designed for a desktop mouse.

In this study, we use an optical sensor as a position estimation device for a mobile robot on a slippery terrain for different distances between the sensor and the terrain surface. To make the system compact and applicable to measurements from large heights, the original lens system and pinhole cover part, designed for a desktop mouse, are not used in our sensing device. We have also designed the device to track different surfaces robustly by using dual laser sources. Moreover, the optical sensor that we chose detects motions with a comparatively higher speed than conventional optical sensors.

In this paper, we first present the laser speckle principle and our sensing device design in section II. Then, we report the performance of the device with dual laser sources in section III. Finally, we introduce some position estimation results for a mobile robot using the device to examine its performance.

## II. SENSING DEVICE

### A. Laser speckles

Our noncontact position estimation device uses a methodology to track the laser speckle pattern (LSP). This is caused by the interference of coherent laser rays reflected from a rough surface with different heights that are much larger than the wavelength of the laser light. The LSP and its applications have been presented elsewhere in detail [14].

An LSP can be seen by a sensor either through a lens or without a lens. If enough space for a lens is available in a robot, a combination that includes a telecentric lens is appropriate for height-invariant measurement [15]. The movements of an LSP can be detected not only by the image sensor in a camera [16] but also by the optical sensor used for computer mice [17].

The motion of an LSP at a sensing plane depends on the distances of the sensor and light source to the surface on which its spot is located [14]. A larger parallelism for the laser beam results in a higher invariability against distance changes. In addition, the average diameter of the LSP changes according to both the distance and diameter of the light spot [18].

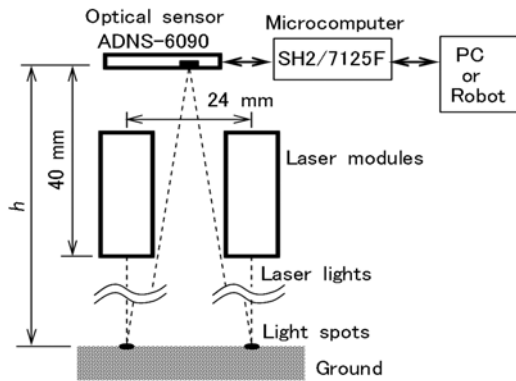


Fig. 1. Distances between the optical sensor, ground, and laser modules in sensing device.

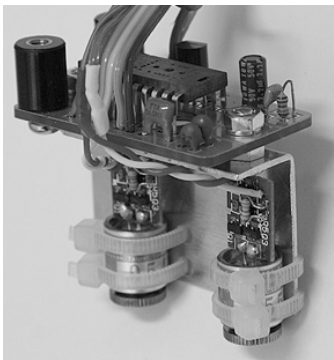


Fig. 2. Optical sensor and two laser modules.

It is difficult to precisely determine the parallelism of the laser beam and the diameter of the laser spot we use. Therefore, we intend to experimentally examine the sensor device while changing conditions such as the distance between the sensor and the surface in this paper.

### B. Functioning scheme of sensing device

The schematic of the sensing device we have developed is shown in Figs. 1 and 2. We use an Avago ADNS-6090 [19] as an optical sensor and two laser modules emitting red beams at a wavelength of 650 nm. The laser module has a lens that allows it to emit an almost parallel beam by a laser diode. Visual observation shows that the diameter of the laser spot is 3.7 mm when the distance is from 70 mm to 500 mm. The sensor device has a maximum velocity of 65 ips (inches per second) and a resolution of 3000 cpi (counts per inch) with the normal lens system recommended by the manufacturer. The actual maximum velocity and resolution properties without the recommended lens are experimentally investigated in section III. The sensor device calculates the relative displacements in the  $X$ - and  $Y$ - directions in a frame period. These displacements of  $\Delta X$  and  $\Delta Y$  are sent to a microcomputer to derive the two-dimensional position using a 0.2-ms frame time. A mobile robot can read the relative position displacement from the microcomputer anytime to estimate its position.

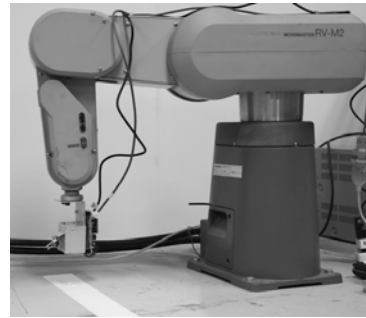


Fig. 3. Experiment environment. A robot arm moves the sensing device in a specified direction with accuracies of 0.1 mm in position and  $0.1^\circ$  in posture.

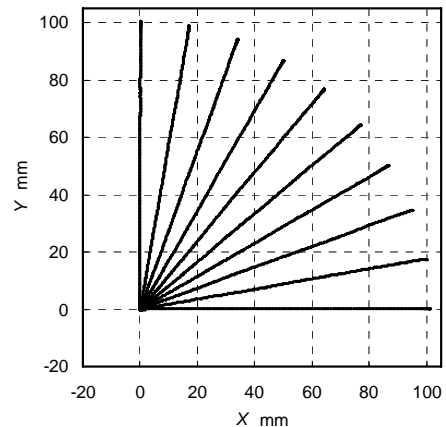


Fig. 4. Measurement result obtained by moving sensing device from origin in different directions.

## III. FUNDAMENTAL PERFORMANCE TESTS FOR DEVICE

Some tests were conducted to evaluate the fundamental performance of the sensing device used to estimate a robot's position. To evaluate the measurement accuracy of the device, its resolution was preliminarily determined by moving the device by a robot arm, *Mitsubishi RV-M2*, as shown in Fig. 3. The resolution was 288 cpi when the device was translated 200 mm in the  $Y$ -direction at a velocity of 50 mm/s and a height of 100 mm on a white paper with dual laser sources.

### A. Translation in plane

The first test was the measurement of the translation displacement in a plane at a constant height. Fig. 4 shows the loci measured when the sensing device was moved 100 mm from the origin at a velocity of 50 mm/s to 10 different positions on a white paper by the robot arm. The average position error of the end points was 0.6% and the maximum position error was 1.5%. The device measured the planar displacement of the object surface with almost constant accuracy independent of the direction of motion.

### B. Different heights

The second test was a comparison measurement of the translation error with different heights and different laser source numbers. The sensor was translated 200 mm in the

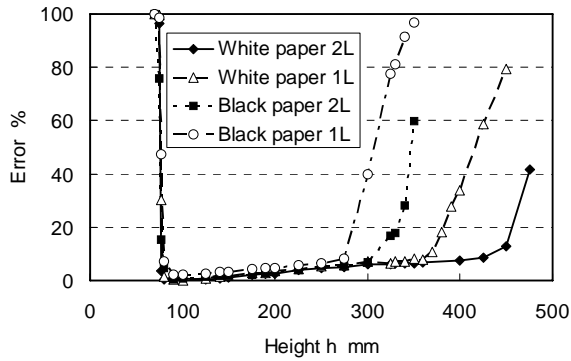


Fig. 5. Measurement errors for different distances between sensor and surface. White and black papers were used in the experiment. 2L and 1L indicate the number of laser sources used.

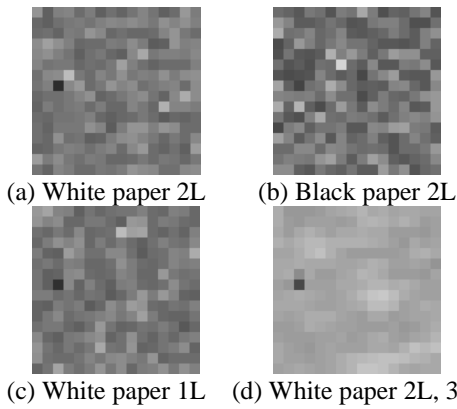


Fig. 6. Image frames captured by the sensor. The distance between sensor and surface is 100 mm for (a)-(c), 300 mm for (d). 2L and 1L mean the number of laser source used. A dark pixel at left-middle in every frame is due to the defect of the sensor.

Y-direction at a velocity of 50 mm/s, at a specified height,  $h$ , above the surface. Two surface colors were used: white and black. The measurement precision at different heights is shown in Fig. 5. In this figure, 1L and 2L indicate the number of laser light sources. The error gradually increases according to the height, and suddenly escalates at a certain height. The sensor covered the widest height range on white paper with dual laser sources because this provided the strongest reflection of the light spots.

The capability of being used for a wide range of heights enables a robust positioning for mobile robots traversing loose or slippery terrains, which cause their wheels to sink. Fig. 5 shows that the measurement error remained within 5% at heights between 100 mm and 200 mm.

The contribution of the dual laser sources is also seen from a comparison of the surface quality (SQUAL) values. The SQUAL value represents the number of valid features visible to the sensor. A higher SQUAL contributes the tracking robustness to the sensor device. The SQUAL values at a height of 300 mm and the conditions of white paper with 2L, white paper with 1L, black paper with 2L, and black paper with 1L were 76, 53, 34, and 30, respectively. The SQUAL with dual laser sources was larger than that with a single laser

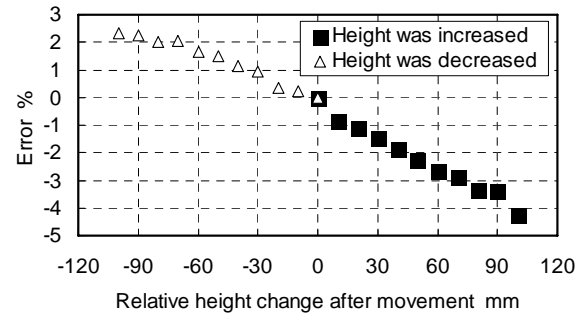


Fig. 7. Measurement error for different heights during 200-mm translation in Y-direction.

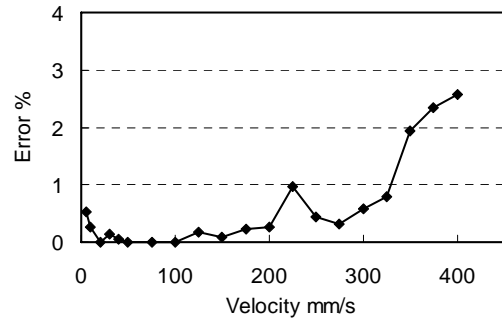


Fig. 8. Absolute error at different velocities.

source. Low SQUAL values below 30 caused large displacement errors.

Fig. 6 shows the image frames captured by the sensor. The images in Figs. 6(a)–(c), taken at a height of 100 mm, have visible clear features and a higher surface quality than the image in Fig. 6(d), which was taken at a height of 300 mm. The feature patterns are almost the same in the frame images taken under different conditions for the number of laser sources. The larger height made the features obscure, which was caused by the weaker luminance of the laser.

### C. Height changes during translation

The third test was for the measurement error of translation in a case where the sensing height was gradually changed. The wheels of a mobile robot typically sink into loose soil during movement. This would cause gradual changes in the height of a sensor mounted on the robot. Therefore, the measurement results from the device need to be stable when the distance between the sensor and the ground changes. Fig. 7 shows the result when the height of the sensor position gradually changed during a 200-mm displacement in the Y-direction. It shows that the amount of absolute error rose slightly from both increases and decreases in the height within 100 mm. However, the amount of this error was less than 5% under these conditions.

### D. Different velocities

The fourth test was for the measurement error of translation in the case of fast speed. Fig. 8 shows the absolute error results when the robot arm moved the sensing device

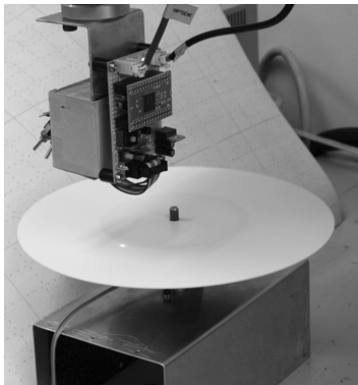


Fig. 9. Turntable driven by motor for measuring maximum velocity of tracking.

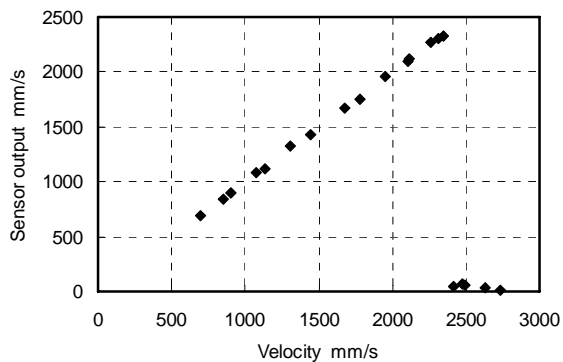


Fig. 10. Result of sensor output for surface moving at very high speed with sensor placed on plastic plate rotated by turntable.

200 mm at a specified velocity, at a height of 100 mm over a white paper. The measurement error was introduced under the conditions of high velocity, acceleration, and deceleration. The measurement accuracy reduced for high-velocity motions. However, the maximum error was less than 3% when the velocity was 400 mm/s.

#### E. Maximum velocity supported

The fifth test was the measurement of the maximum velocity supported by the device. The sensor was fixed on a steady robot arm, and the surface of a plastic plate was turned by an actuated turntable, as shown in Fig. 9. The rotational speed was calculated with the pulse period of a photointerrupter under the turntable. The velocity of the surface could be estimated using both the rotation rate and the radius of the sensor position. As shown in Fig. 10, the maximum velocity that can be measured by the sensing device was 2300 mm/s (approximately 8.3 km/h), which is sufficient for conventional outdoor mobile robots, including our robot.

#### F. Different surface materials

The sixth test was for the measurement capability in the case of different surface materials. Fig. 11 shows the error in the Y-direction estimated by the device after it traveled 200

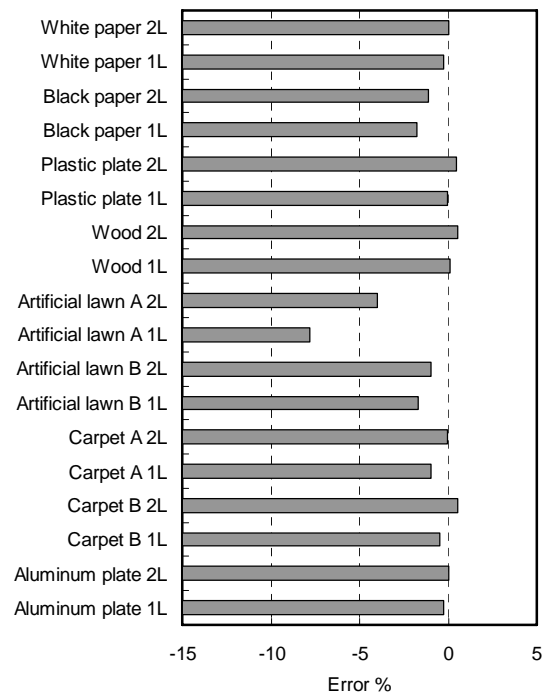


Fig. 11. Measurement error of proposed device for 200-mm displacement on different surface materials. 2L and 1L indicate the number of laser sources used.

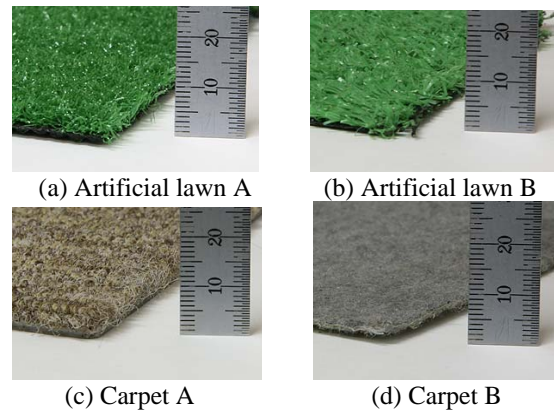


Fig. 12. Some examples of various surface materials used in experiment.

mm in the Y-direction at a velocity of 50 mm/s and a height of 100 mm. The differences between the graphs for A and B are due to the thicknesses of the materials. Artificial lawn A and carpet A were thicker than artificial lawn B and carpet B, respectively, as shown in Fig. 12. The labels 2L and 1L in the figure indicate the number of laser sources turned on for the device. The dual laser sources made the tracking more robust against different surface materials compared to the single source, particularly in the results for artificial lawn A. Artificial lawn A greatly reduced the luminance of the laser spot, so that the sensor struggled with tracking. The device could estimate motions even on patternless surfaces such as paper, plastic plates, and aluminum plates. The absolute error

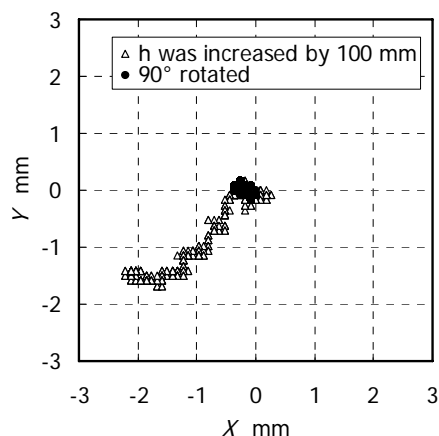


Fig. 13. Measurement results for sensor moved 100 mm in height direction and rotated 90° along Z-axis.

of the device with dual laser sources was less than 4% over different surfaces.

#### G. Movements unsupported by the device

The seventh test was used to determine the measurement behavior in a case where the sensor was moved in unsupported ascent and rotation directions. Fig. 13 shows the measured positions when the robot arm moved the sensing device with two types of motions. In the first, only the height was changed by 100 mm, while in the other, the device was rotated by 90° with the position fixed. The rotation of the sensor was produced by a rotation of the wrist joint of the robot arm. The device output was fairly small when it was moved in the height direction, while the sensor output was large when it was rotated. These experimental results indicate that the device can hardly estimate a movement that it was not designed to support.

#### IV. MEASURING ON SLIPPERY TERRAIN

From the above performance tests, we concluded that the device is reasonably effective at estimating a robot's position. Therefore, we mounted it on our mobile robot and evaluated the performance of the sensing device in loose soil.

The sensing device was installed on the body of a rover vehicle that was developed by our research group. This vehicle is 810 mm in length, 510 mm in width, 430 mm in height, and has a weight of approximately 24 kg. The diameter of the wheels is 100 mm. The optical sensor was attached 150 mm above the ground surface.

We conducted traversing experiments with the rover on an inclined sandy slope, as shown in Fig. 14. The rotational velocity of the four driving wheels was set at 7.5 rpm, giving the rover a speed of 40 mm/s without slippage. Two laser spots can be seen near the rear-left wheel in this figure. The rover gradually sank up to 30 mm into the loose terrain with large slippage while traversing this terrain, thus degrading the reliability of wheel odometers for the rover.

Table 1 shows the actual displacement as measured by a

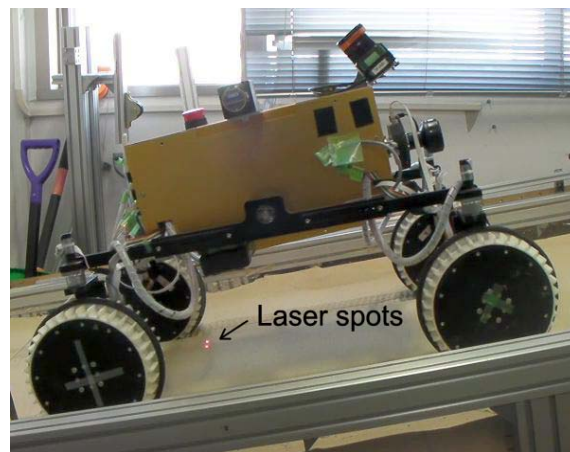


Fig. 14. Rover vehicle with proposed sensing device climbing 10° inclined sandy terrain.

Table 1. Absolute error in displacement estimated by conventional odometer and proposed sensing device on sandy terrain inclined at 10°.

Trial	Actual [mm]	Absolute error [%]	
		Mechanical odometer	Proposed sensing device
1	1030	37.9	3.9
2	950	40.0	1.1
3	970	37.1	0.0
Average		38.3	1.7

Table 2. Absolute error in displacement estimated by conventional odometer and proposed sensing device on sandy terrain inclined at 12°.

Trial	Actual [mm]	Absolute error [%]	
		Mechanical odometer	Proposed sensing device
1	970	175.3	1.0
2	910	193.4	2.2
3	900	163.3	3.3
Average		177.3	2.2

scale and the estimation errors of a wheel odometer and the proposed sensing device as the rover climbed a sandy slope with an inclination of 10°. The average measurement error of the wheel odometer was 38.3%, while that of the sensing device was 1.7%. Table 2 shows the measurement results when the slope inclination was 12°. The rear wheels of the rover slipped much more than in the case of the 10° slope. The average measurement error of the wheel odometer was 177.3%, while that of the sensing device was 2.2%, which was considerably much better than the wheel odometer.

These results prove that the sensing device we have developed provides more robust odometry against wheel slippage and sinkage in a mobile robot than the conventional wheel odometer.

## V. CONCLUSION

In this paper, we have presented a sensing device that uses an optical sensor, designed for a computer mouse, and dual laser light sources to estimate the position of a robot traversing slippery terrains.

First, we explained laser speckles, which are used for noncontact sensing at a large distance from the ground surface. Second, we presented our developed sensing device and investigated its performance robustness against different surfaces and height changes by moving the device using a robot arm. The results of this experiment showed that the measurement error remained within 5% at heights between 100 mm and 200 mm. Another experiment showed that the maximum velocity of the sensing device was 2300 mm/s (approximately 8.3 km/h), which is sufficient for a conventional mobile robot. Moreover, the absolute error of the device with dual laser sources was less than 4% for different surfaces. Third, we introduced our simple results to show that our mobile robot can traverse even loose soil. The precision of the position estimated by the proposed device was considerably higher than that of the wheel odometry on the slippery terrain. The average measurement error of the sensing device was 2.2% in the experiment with our rover vehicle.

This sensing device is so compact, inexpensive, and simple that it can be easily used in mobile robots for estimating their position. Since, in principle, the device does not estimate the rotational displacement caused by a posture change in a mobile robot, other sensors are required to estimate the rotational displacement, for example gyroscopes. Using many such sensing devices, including laser sources, may improve the estimation accuracy of a mobile robot's position or enable three-dimensional odometry.

## ACKNOWLEDGMENT

This work was supported by a Grant-in-Aid for Scientific Research (B) 21360110.

## REFERENCES

- [1] J. Palacin, I. Valganon, and R. Pernia, "The optical mouse for indoor mobile robot odometry measurement," in *Sensors and Actuators A*, vol. 126, 2006, pp. 141–147.
- [2] U. Minoni and A. Signorini, "Low-cost optical motion sensors: An experimental characterization," in *Sensors and Actuators A*, vol. 128, iss. 2, 2006, pp. 402–408.
- [3] F. Santos, V. Silva, and L. Almeida, "A Robust Self-localization System for a Small Mobile Autonomous Robot," in *Proc. of the 2002 IEEE International Symposium on Robotics and Automation*, 2002.
- [4] D.K. Sorensen, V. Smukala, M. Ovinis, and S. Lee, "On-line Optical Flow Feedback for Mobile Robot Localization/Navigation," in *Proc. of the 2003 IEEE/RSJ International Conference on Intelligent Robots and Systems*, 2003, pp. 1246–1251.
- [5] S. Lee and J. Song, "Mobile robot localization using optical flow sensors," in *International Journal of Control, Automation, and Systems*, vol. 2, iss. 4, 2004, pp. 485–493.
- [6] M. Tresancheza, T. Pallejaa, M. Teixidoa, and J. Palacin, "The optical mouse sensor as an incremental rotary encoder," in *Sensors and Actuators A*, vol. 155, 2009, pp. 73–81.
- [7] S. Lee and J.-B. Song, "Robust mobile robot localization using optical flow sensors and encoders," in *Proc. of the 2004 IEEE International Conference on Robotics and Automation*, 2004, pp. 1039–1044.
- [8] X.-m. Tan, D. Zhao, and J. Yi, "A novel pose estimation system for indoor mobile robots based on two optical sensors," in *Lecture Notes in Control and Information Sciences*, vol. 362, 2007, pp. 41–50.
- [9] A. Bonarini, M. Matteucci, and M. Restelli, "Automatic Error Detection and Reduction for an Odometric Sensor based on Two Optical Mice," in *Proc. of the 2005 IEEE International Conference on Robotics and Automation*, 2005, pp. 1675–1680.
- [10] J. A. Cooney, W. L. Xu, and G. Bright, "Visual dead-reckoning for motion control of a Mecanum-wheeled mobile robot" in *Mechatronics*, vol. 14, iss. 6, 2004, pp. 623–637.
- [11] J.D. Jackson, D.W. Callahan, and J. Marstrand, "A Rationale for the use of Optical Mice Chips for Economic and Accurate Vehicle Tracking," in *IEEE International Conference on Automation Science and Engineering*, 2007, pp.939–944.
- [12] S.P.N. Singh and K.J. Waldron, "Design and evaluation of an integrated planar localization method for desktop robotics," in *Proc. of the 2004 IEEE International Symposium on Robotics and Automation*, 2004.
- [13] O. Maye, J. Schaffner, and M. Maaser, "An Optical Indoor Positioning System for the Mass Market," in *Proc. of the 3rd Workshop on Positioning, Navigation and Communication*, WPNC'06, 2006, pp. 111–116.
- [14] I. Yamaguchi, "Theory and applications of speckle displacement and decorrelation," in *Speckle Metrology*, edited by R.S. Sirohi, Marcel Dekker, Inc., New York, 1993, pp. 1–39.
- [15] N. Tunwattanaa, A.P. Roskillya, and R. Normanb, "Investigations into the effects of illumination and acceleration on optical mouse sensors as contact-free 2D measurement devices," in *Sensors and Actuators A*, vol. 149, iss. 1, 2009, pp. 87–92.
- [16] C.-M. Liao, P. S. Huang, Y.-Y. Hwang, M. Chen, and C.-C. Chiu, "Robust technique of analyzing and locating laser speckle patterns for optical computer mice," in *Optics and Lasers in Engineering*, vol. 47, iss. 7-8, 2009, pp. 875–883.
- [17] T.W. Ng and M. Carnea, "Optical mouse digital speckle correlation," in *Optics Communications*, vol. 280, iss. 2, 2007, pp. 435–437.
- [18] P. Popov, S. Pulov, and V. Pulov, "A laser speckle pattern technique for designing an optical computer mouse," in *Optics and Lasers in Engineering*, vol. 42, iss. 1, 2004, pp. 21–26.
- [19] Avago, ADNS-6090 Gaming Laser Mouse Sensor Data Sheet, <http://www.avagotech.com>, 2008.